



Optimizing the Mechanical Properties of AS21 Magnesium Alloy/SiC-TiO₂ Hybrid Composites by Taguchi Method

Srinivas Chandanam^{1*}, Ramgopal Reddy Bijjam¹, N. V. V. S. Sudheer¹, Rognatha Rao Dasi²

¹ Department of Mechanical Engineering, R.V.R. & J.C. College of Engineering, Chowdavaram, Guntur 522019, India

² Department of Mechanical Engineering, SRK Institute of Technology, Enikepadu, Vijayawada 521108, Andhra Pradesh, India

Corresponding Author Email: srinivaschandana2010@gmail.com

Copyright: ©2025 The authors. This article is published by IIETA and is licensed under the CC BY 4.0 license (<http://creativecommons.org/licenses/by/4.0/>).

<https://doi.org/10.18280/rcma.350113>

ABSTRACT

Received: 9 December 2024

Revised: 14 January 2025

Accepted: 12 February 2025

Available online: 28 February 2025

Keywords:

AS21/SiC-TiO₂ hybrid composites, taguchi method, mechanical properties, stir-casting, ANOVA, material science, composite optimization, mechanical testing

Magnesium metal matrix composites are extensively utilized in lightweight applications particularly in aeronautical, automotive and biomedical fields. Therefore, it's essential to develop an optimal combination of multi-response process parameters to enhance the mechanical characteristics of these composites. This research employs the Taguchi method to identify the best configurations of process variables for producing AS21/SiC-TiO₂ hybrid composites. The AS21 alloy hybrid composites were produced using stir-casting, considering input process parameters such as weight % of SiC, TiO₂, melt temperature and stirring rate by varying each parameter at 3 levels using Taguchi L27 Orthogonal Array. Hardness and tensile strength were assessed as the response characteristics of AS21 hybrid composites. The results depict that the highest hardness of 94HV was achieved with optimized parameters: temperature of melt 750°C, speed of stirring 400rpm, and reinforcements of 2 wt% Silicon Carbide (SiC) and 0.5 wt % Titanium Dioxide (TiO₂). For tensile strength, the optimal parameters resulted in a maximum strength of 253MPa, using the same melt temperature and stirring speed, but with 3 wt% SiC and 0.5 wt% TiO₂. The findings indicate that the Taguchi method is a reliable approach for determining optimal manufacturing parameters to improve the properties of AS21/SiC-TiO₂ hybrid composites. The Taguchi optimization showed minimal variation, with an error of just 1.64%, indicating strong consistency. ANOVA was performed to validate the model and identify the most significant parameters. The results revealed that hybrid reinforcement has the most substantial impact on the performance of the cast AS21/SiC-TiO₂ hybrid composites. These optimized composites hold significant potential for high-performance applications, such as brake linings, light weight armor plates for military vehicles, engine blocks, cylinder heads, pistons and heat sink for electronic devices where factors like durability, strength, and wear resistance are essential.

1. INTRODUCTION

Magnesium (Mg) alloys are gaining prominent attention for their wider applications in the aeronautical and automobile sectors due to their remarkable properties. Furthermore, magnesium metal matrix composites are known for their excellent castability, thermal stability, machinability, and damping characteristics [1, 2]. Because of magnesium alloy strong attraction to oxygen, the synthesis and production of Mg metal matrix materials is a major issue for academics and scientists. The casting process has gained popularity for producing Mg alloy composites for structural applications [3, 4]. High grade defense and aerospace components are manufactured using permanent mold and gravity sand casting [5]. Due to its near net form components and cost-effectiveness, stir-casting of magnesium alloy composites in a vacuum aided argon atmosphere is one of the

sustainable techniques [6]. The studies [7, 8] researched the Pure Mg, Mg-TiO₂, Mg-TiC and Mg-TiN composite material using DMD process. The results showed that a small addition of (TiO₂/TiC/TiN) reinforcement to the magnesium matrix led to an enhancement in mechanical properties, without influencing the Young's modulus or cytotoxicity, which remained comparable to that of human bone.

The stiffness, strength and hardness of Mg AS21 alloy amalgamated with ceramic reinforcements are improved [9]. The characteristics of the composite are dramatically changed by homogeneous reinforcement dispersion in the Mg matrix [10]. In this context, various ceramic reinforcements such as B₄C, Al₂O₃, TiB₂ and SiC have been identified to enhance the Mg alloys properties [11-13]. A few combinations of reinforcements had a substantial impact on how well composites performed. For instance, Aathisugan et al. [14] examined the features of B₄C and graphite reinforced into

AZ91D Mg hybrid composites and found that increased weight percentages of these materials enhanced both hardness and tensile properties. The authors also noted a significant improvement in wear resistance due to the addition of B₄C-graphite reinforcement. Tensile, compressive and wear behaviour of self-lubricating sintered magnesium-based composites were examined by Narayanasamy and Selvakumar [15]. Their findings revealed that adding Gr and MoS₂ enhanced the composites tensile strength and hardness. Karthick et al. [16] investigated microstructure and mechanical properties of Al₂O₃ and SiC reinforced magnesium metal matrix hybrid composites. They found that incorporating SiC improved the composite tensile strength and hardness.

In recent years, researchers have used Taguchi Design of Experiments (DOE) to pinpoint the important variables affecting the features of metal matrix composites (MMCs). The ideal powder metallurgy and stir casting manufacturing parameters for magnesium composites were investigated and optimized by Rognatha Rao and Srinivas [17] and Balak and Zakeri [18] for magnesium composites, focusing on casting duration, temperature and reinforcement volume. For AA6063/SiC composites, Babu and Jeyapaul [19] improved wear parameters, concluding that the Taguchi approach enhances friction wear behavior under ideal experimental conditions. Elumalai et al. [20] investigated the physical, microstructural and mechanical behavior of titanium dioxide nanoparticulate reinforced magnesium composite. The authors came to the conclusion that hybrid reinforcement reduces the wear rate of AZ91 composite. In order to enhance the characteristics of Mg-TiO₂ composites produced by stir-casting Meenashisundaram et al. [21] investigated and developed the high-performance Mg-TiO₂ nanocomposites targeting for biomedical/structural applications using the ideal parameters by Taguchi method and identified the significant variables such as duration of stirring, speed of stirring and reinforcing percentage for enhancing the properties of composite. Meenashisundaram et al. [22] investigated the effects of primary processing techniques and significance of hall-petch strengthening on the mechanical response of magnesium matrix composites containing TiO₂ nanoparticulates. Because of their high hardness, stiffness, good thermal stability, relatively low density, and capacity to effectively impede dislocation movement within the magnesium matrix, SiC and TiO₂ are often employed as reinforcement materials in magnesium alloys. This results in notable improvements in the wear endurance and material strength of the resulting composite material.

In the previous studies only process variables, such as stirring speed and temperature, were used, and obtained satisfactory results on materials other than the AS21/SiC-TiO₂.

The present study aims to find the optimal stir-casting process variables for AS21/SiC-TiO₂ hybrid composites such as the melt temperature, stirring rate, weight % of SiC and TiO₂ reinforcements at three distinct levels are considered. To achieve the ideal level of the process variables, the impact of these parameters on response features of strength and hardness are examined using Taguchi L27 orthogonal array.

2. FABRICATION PROCEDURE

The nominal composition of the readily available AS21

magnesium alloy ingot (Mg-3Al-0.98, Zn-0.2Mn) was chosen as the base matrix and SiC and TiO₂ were used as reinforcements. Table 1 shows the several compositions designed for AS21/SiC-TiO₂ hybrid composites.

A predetermined amount of the AS21 magnesium alloy was melted down in an induction furnace at 650°, 700°, and 750°C in an inert atmosphere. SiC and TiO₂ particles in a known quantity were precisely measured and added to the melt of the magnesium alloy to create the Mg hybrid composite. In order to eliminate water content from particles and improve wettability in a matrix material, the hybrid reinforcements are usually pre heated in a muffle furnace.

To eliminate the entrapped gases and stop reaction with oxygen in the melted metal in the melting operation, a cover flux containing 1% matrix was utilized. At consistent periods, an impeller churned the composite melt continuously. Three different stirring speeds were used: 600, 500 and 400rpm.

Table 1. Chemical make-up of hybrid composites made of AS21/SiC-TiO₂

SiC (Wt. %)	TiO ₂ (Wt. %)	AS21 (Wt. %)	Composite Designation
2	0.5	97.5	AS21+2 SiC+0.5 TiO ₂
3	0.5	96.5	AS21+3 SiC+0.5 TiO ₂
4	0.5	95.5	AS21+4 SiC+0.5 TiO ₂
2	1.0	97.0	AS21+2 SiC+1.0 TiO ₂
3	1.0	96.0	AS21+3 SiC+1.0 TiO ₂
4	1.0	95.0	AS21+4 SiC+1.0 TiO ₂
2	1.5	96.5	AS21+2 SiC+1.5 TiO ₂
3	1.5	95.5	AS21+3 SiC+1.5 TiO ₂
4	1.5	94.5	AS21+4 SiC+1.5 TiO ₂

2.1 Fabrication of MMCs using stir casting method

The metal matrix composite is created in liquid state by incorporating dispersion phases into the molten matrix metal and settling it. In order to obtain a high mechanical performance of a composite, it is important to have a good interfacial bond (wet) between dispersed phase and liquid matrix. In stirred metal casting process, a stirrer is used to generate a swirl in mixing reinforcement and matrix. It is an efficient method to manufacture of MMCs because it is cheap, adapted to mass production, simple, near-network shaped and easy to manage the composite structure.

2.2 Stir casting setup

Figure 1 shows that the experimental stir casting setup and its parts.



Figure 1. Stir casting machining setup

2.3 Specifications of stir casting

- Capacity of Furnace-2kg.
- Temperature limit $\leq 1000^{\circ}\text{C}$.
- Mechanical Stirrer ranging from 0 to 1000 rpm, blade made of stainless steel.
- Proportional-Integral-Derivative based Temperature Control.
- Dies made of mild steel of i) diameter 30mm and Lenth 300mm ii) diameter 20mm and length 150mm.

Coating the dispersed phase's fibres can promote wetting. A good coating reducing interfacial energy while also blocking chemical interactions between matrix and dispersed phase. Stir casting are most simple and cost-effective method of making liquids.

The melted composite was then flowed in a heated cylindrical mold of gray cast iron, which was given some time to cool. To remove any remaining tensions, the Mg alloy composite underwent a 12-hour homogenization process. The cast specimens are shown in Figure 2.

The AS21 hybrid composite specimens were prepared through machining for mechanical testing and microstructural examination which are made according to ASTM standards. Microstructure analysis was conducted using optical microscopy and SEM. The micro-hardness of different areas on the periphery of the composite was evaluated at a load of 100 g and a dwell time of 10 seconds. According to ASTM E-8 standard, calculation of tensile strength is done by a computerized Universal Strength Testing Machine at a ram speed of 3 mm/min and ambient temperature. Using the Taguchi L27 technique, the processing parameters for AS21/SiC-TiO₂ hybrid composites were optimized. Degrees of variance in the control factors used in this research are shown in Table 2.



Figure 2. Cast specimens of AS21/ SiC-TiO₂ hybrid composites

Table 2. Control factors and investigation ranges

Parameters	Level 1	Level 2	Level 3
Temperature of Melt (T _m) in °C	650	700	750
Stirring Speed (S) in rpm	400	500	600
Weight % Silicon carbide (SiC)	2	3	4
Weight % Titanium oxide (TiO ₂)	0.5	1	1.5

The purpose of the Taguchi method is to decrease process variation through robust design of experiments. Its primary aim is to deliver high-quality products at a price that is affordable for the producer. Taguchi proposed an experimental design in which the process parameters and their appropriate levels are arranged using orthogonal arrays. Unlike the factorial design, which requires testing every conceivable combination, the Taguchi approach just evaluates pairs of combinations. This makes it possible to get the information required to identify the variables that have the most impact on product quality with minimum number of experiments in less time and money. When there are few interactions between variables, only a small number of variables significantly affect the outcome, and there are between three to fifty variables, the Taguchi approach works well.

3. RESULTS AND DISCUSSION

3.1 Hardness variations

Hardness variations for AS21/SiC-TiO₂ composites in different compositions were shown in Figure 3. The hardness of AS21 alloy was measured at the fusion temperature 750°C and stirring speed 600 rpm.

However, in AS21 base matrices, with 2% SiC added, the hardness increased by 10.67% and 4% SiC added by 18.75%. The incorporation of SiC reinforcement greatly enhances the hardness. The reduction in local deformation in plastic caused by distribution of the Silicon Carbide particles in the notch leads to improved hardness.

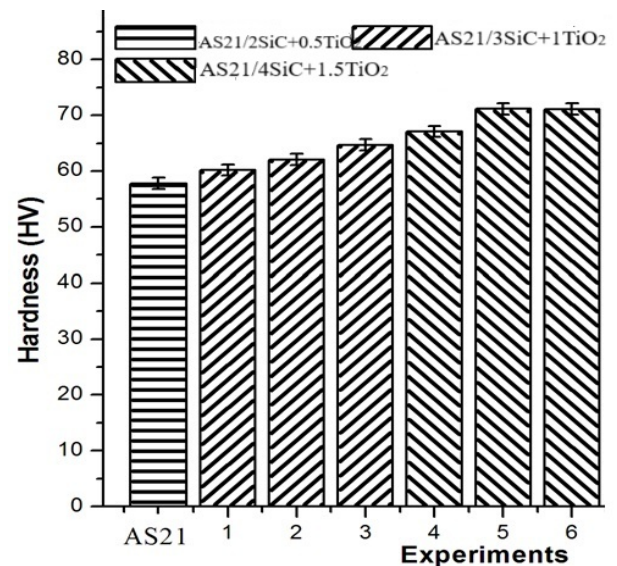


Figure 3. SiC-TiO₂ reinforcement effect for hardness of AS21 Mg composites

3.2 Tensile strength variation

The tensile strength of the AS21 Mg alloy is 141.69MPa. When 1.5% TiO₂ and 2% SiC were added to the AS21 Mg alloy, the tensile strength increased to 159.31 MPa. As the SiC content was raised from 2% to 3%, the tensile strength improved to 170.51MPa. Finally, with an increase in Silicon Carbide from 2% to 4%, the tensile strength reached 199.35

MPa. Figure 4 illustrates the stress-strain curves of the Mg-SiC-TiO₂ metal matrix composite during tensile testing at different intervals.

As a result, the SiC-TiO₂ reinforcement led to a 40.69% raise in the tensile strength of the AS21 alloy. The structure with 4% SiC reinforcement, along with robust interfacial interactions between the reinforcement and the matrix, enhanced the tensile strength of AS21 alloy.

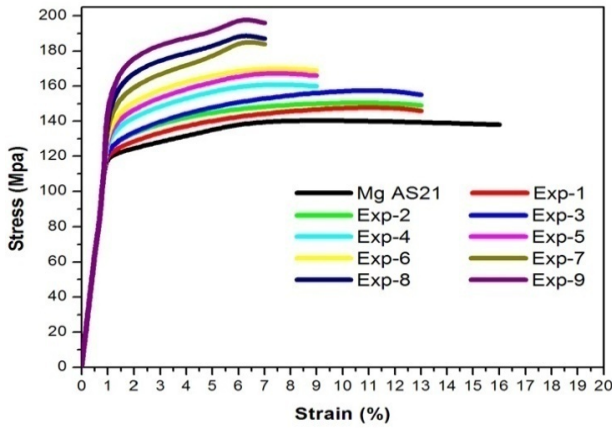


Figure 4. Stress-strain curves of AS21 Magnesium composites

3.3 Porosity analysis

A magnesium metal matrix composite (MMC) porosity analysis report would detail the evaluation of void content (porosity) in a magnesium-based composite. This typically examining the distribution, size and volume percentage of pores, often using methods like Optical Microscopy and

scanning electron microscopy (SEM) and image analysis software to evaluate the effects of manufacturing process parameters on the structural integrity and mechanical characteristics of the composite material. Key aspects to be included in the report include: sample preparation, porosity measurement methods, porosity distribution analysis, identification of potential causes of porosity, and process optimization recommendations to minimize porosity levels within the magnesium MMC.

Figure 5 illustrates the casting time effects on the relative porosity of the composites. As casting temperature raised from 300°C to 400°C, the porosity ratio of 15% Mg-SiC-TiO₂ composites enhanced by 38.1% at a squeeze pressure of 300 MPa, but reduced by 17.7% at 600 MPa (Figure 5). As casting temperature raised from 400°C to 500°C, the porosity ratio reduced by 38.7% at 300MPa and decreased by 10.2% at 600MPa. For 30% Mg-SiC-TiO₂ composites, increasing the casting temperature from 300°C to 400°C led to a 24.9% increase in porosity ratio at 300MPa, while at 600MPa, the porosity reduced by 1.4% (Figure 5). With a temperature rise from 400°C to 500°C, the porosity ratio in the 30% composites enhanced by 3.3% at 300MPa and increased by 17.2% at 600MPa. From Figure 5, it is evident that in the 15% Mg-SiC-TiO₂ composites, when the casting time was extended from 30 to 60 minutes, the porosity ratio enhanced by 22.4%.

As the casting time was increased from 60 to 90 minutes, the porosity reduced by 21% at a squeeze pressure of 300MPa. A 4% decrease in porosity was observed when the casting time was enhanced from 30 to 60 minutes. In the case of 15% Mg-SiC-TiO₂ composites, the porosity decreased by 3.9% at 600MPa squeeze pressure when the casting time was extended from 60 to 90 minutes. For the 30% Mg-SiC-TiO₂ composites, a 2.1% reduction in porosity ratio occurred when the casting time was enhanced from 30 to 60 minutes.

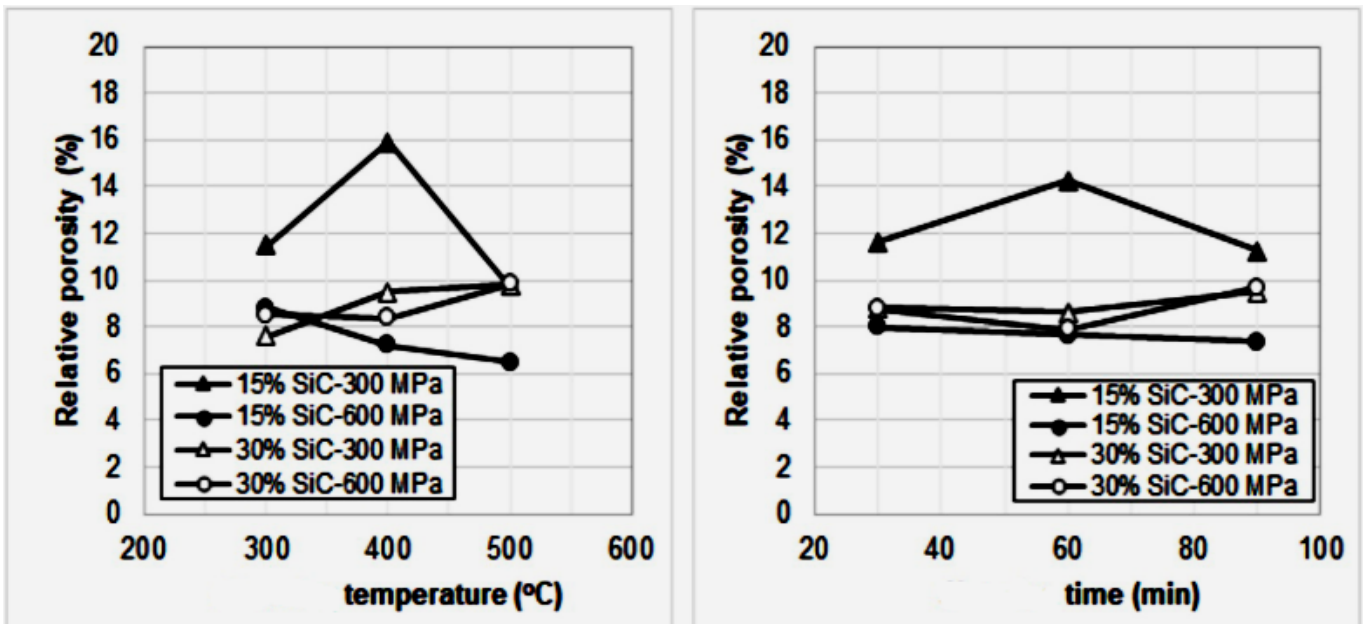


Figure 5. Relative porosity Vs casting temperature and time

3.4 Microstructure

The microscopic images of AS21/SiC-TiO₂ hybrid composites at different process parameter levels is shown in

Figure 6. The AS21 Mg hybrid composite (Figure 6 (a)) exhibits homogenous microstructure when operated at 650°C, 400rpm, 2% SiC, and 0.5% TiO₂. With the following process parameters: 750°C, 600rpm, 3% SiC, and 0.5% TiO₂ (Figure

6 (b)) and 750°C, 400rpm, 3% SiC, and 1% TiO₂ (Figure 6 (c)), similar data were reported. The composite that was created using the 750°C, 400rpm, 4% SiC, and 1.5% TiO₂ (Figure 6 (d)), process conditions, however, displayed an irregular grain structure and microscopic blow holes.

The Scanning Electron Microscope image of the AS21-3SiC+1TiO₂ hybrid composites is shown in Figure 7 (a). The microstructure clearly shows a uniform dispersion of the Silicon Carbide and TiO₂ hybrid reinforcement. In contrast, the AS21+4 SiC+1.5 TiO₂ compositions show agglomerated particles of TiO₂ and SiC reinforcements separating AS21 grains in Figure 7 (b). However, particle aggregation was observed in the microstructure of AS21 samples with 4 wt% SiC and 1.5 wt% TiO₂ reinforcements, independent of the melting temperature and stirring speed. Higher stirring speeds were observed to result in bigger grain sizes and a higher volume fraction of composites during the recrystallization process. Moreover, the layered eutectic phases on the

surfaces of SiC particles broke into refined particles after casting. The influence of refined precipitates on grain boundaries becomes more significant as the particle volume fraction raises and the size of the precipitated phase reduces. This promotes dynamic recrystallization, which is accompanied by an enhanced nucleation rate and the development of refined grains. The dynamic refined recrystallized grains form as a result of the grain growth of the crystalline precipitated phase. Fabricated SiC particle reinforced magnesium metal matrix composites by the stir casting and found that increasing the deformation pass of multi-directional casting allowed additional time and energy for Initiation and expansion of recrystallized grains. Following the casting process, the creation of various crystal defects, such as dislocations and vacancy clusters, provided potential nucleation sites for dynamic recrystallization. Additionally, grain boundaries can serve as sites for nucleation, contributing to further grain refinement.

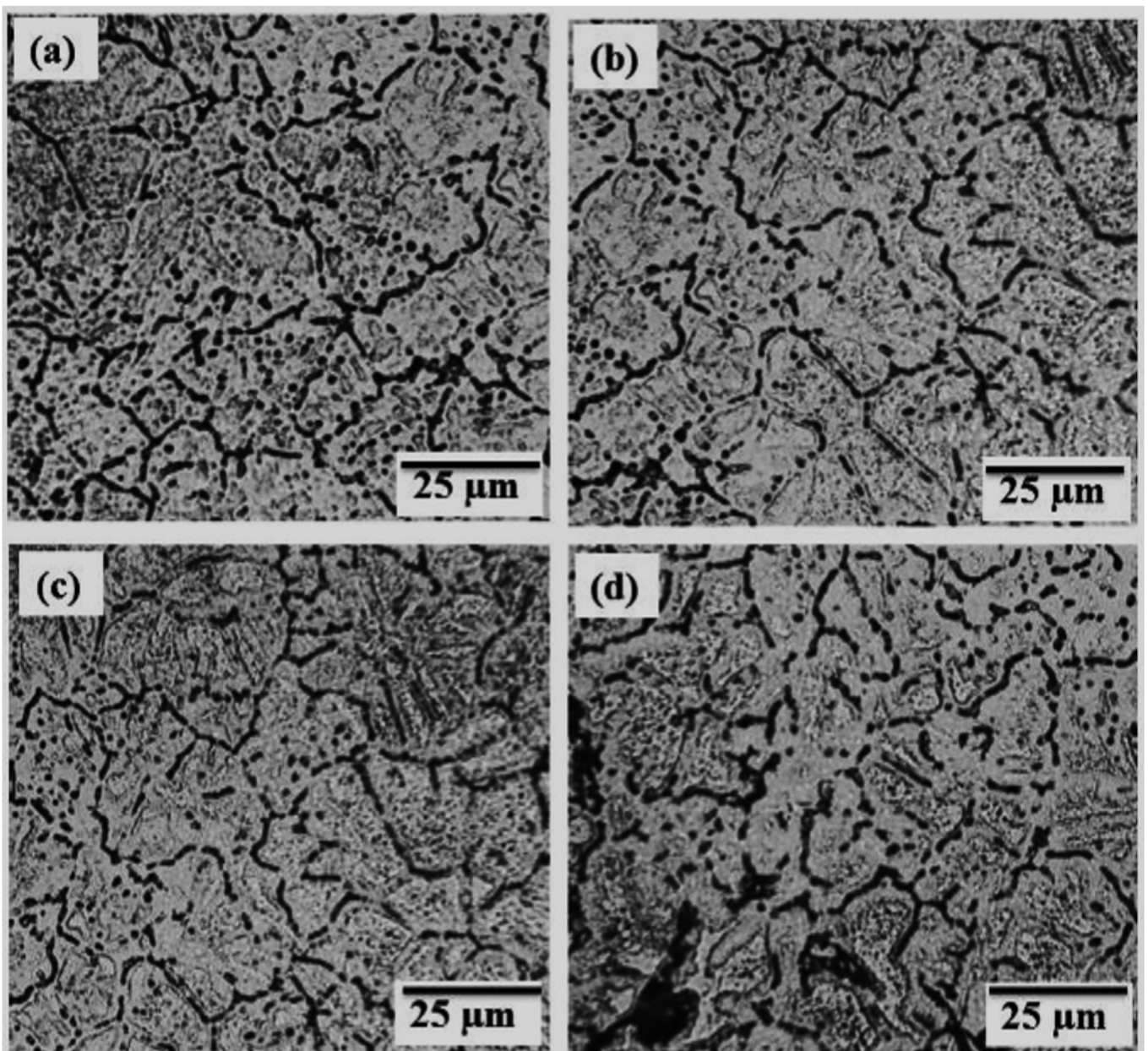


Figure 6. Optical microstructure of AS21 composites at various process parameters

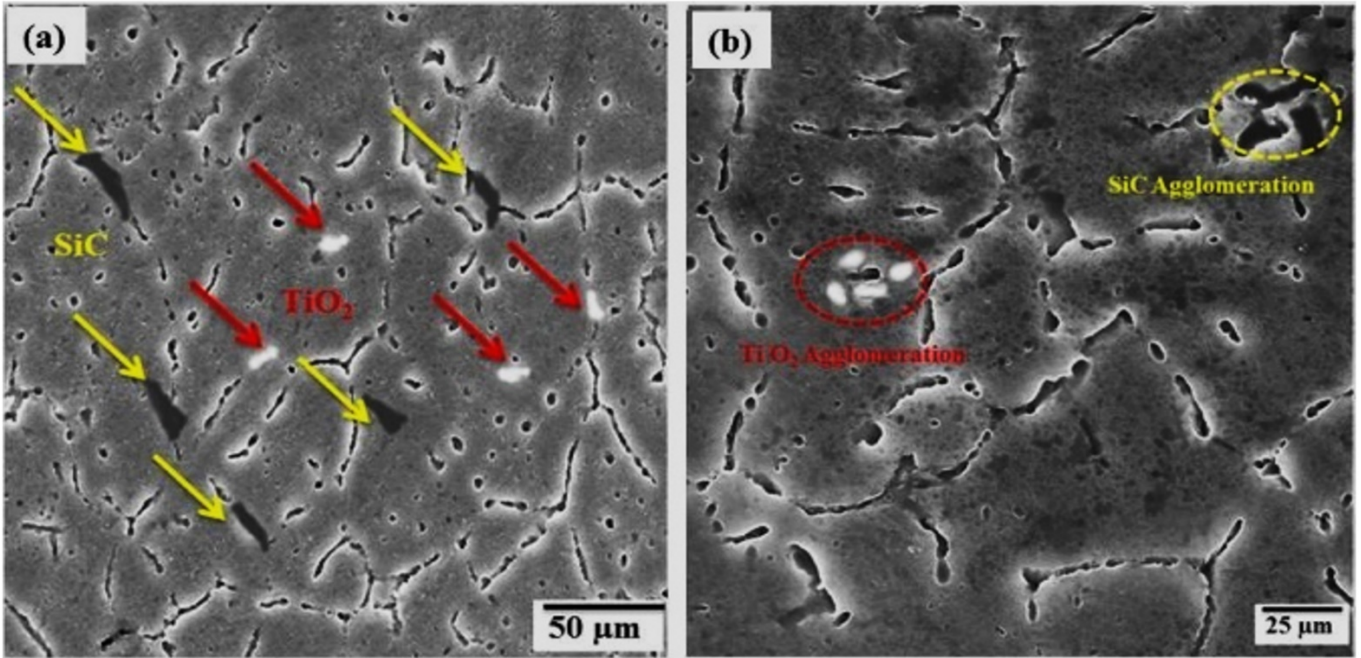


Figure 7. SEM image of (a) AS21+3 SiC+1 TiO₂ (b) AS21+4 SiC+1.5 TiO₂

3.5 Taguchi method

Taguchi method is an effective tool for developing mechanisms using orthogonal array (OA) tests. It offers a streamlined and efficient method for predicting the optimal settings of process control parameters. A typical Taguchi optimization process for parameter design includes several key phases:

Step 1: Identification of objective and quality

characteristics of experiments through pilot study.

Step 2: categorize the most influencing factors, their levels and possible interactions.

Step 3: Selection of suitable orthogonal array (OA) and allocate factors with their levels to OA.

Step 4: Experimental data analysis using S/N ratio and ANOVA analysis.

Step 5: Optimal design parameters verification using confirmation experiments.

Table 3. Taguchi L₂₇ orthogonal array with input and output characteristics

Exp. No	T _m	S	SiC, Wt. %	TiO ₂ , Wt. %	Hardness, HV	S/N Ratio	Strength, MPa	Signal/Noise Ratio
1	650	400	2	0.5	84	39.5856	241	47.8403
2	650	400	3	1.0	86	37.5900	250	48.7588
3	650	400	4	1.5	60	36.6630	203	47.3499
4	650	500	2	1.0	82	36.3763	234	48.5843
5	650	500	3	1.5	63	36.8868	228	47.2587
6	650	500	4	0.5	74	38.4846	221	48.9878
7	650	600	2	1.5	70	37.8020	208	47.5613
8	650	600	3	0.5	85	37.6884	243	48.5121
9	650	600	4	1.0	61	36.6066	214	47.7083
10	700	400	2	0.5	92	38.3758	243	49.6121
11	700	400	3	1.0	88	39.7897	245	48.8833
12	700	400	4	1.5	63	36.8868	204	48.4926
13	700	500	2	1.0	87	39.6904	237	46.6950
14	700	500	3	1.5	63	36.8868	228	46.3587
15	700	500	4	0.5	79	38.8525	225	48.1437
16	700	600	2	1.5	76	38.7163	208	47.2613
17	700	600	3	0.5	87	39.6904	243	48.6121
18	700	600	4	1.0	70	37.8020	216	47.6891
19	750	400	2	0.5	94	38.5626	247	46.9539
20	750	400	3	1.0	82	37.3763	256	47.4648
21	750	400	4	1.5	67	37.4215	199	46.4771
22	750	500	2	1.0	90	38.1849	243	46.8121
23	750	500	3	1.5	79	38.7525	234	48.5843
24	750	500	4	0.5	77	36.6298	228	48.2587
25	750	600	2	1.5	79	36.9525	203	44.3499
26	750	600	3	0.5	87	37.8904	253	47.1624
27	750	600	4	1.0	70	35.8020	208	45.4613

Table 4. Hardness-S/N ratio analysis table

Level	T _m (°C)	S(rpm)	SiC, Wt. %	TiO ₂ , Wt. %
1	38.19	38.81	39.33	37.05
2	36.08	36.78	38.89	36.85
3	37.17	36.67	37.64	35.62
Delta	0.89	0.23	1.59	1.68
Rank	3	4	2	1

Table 5. Tensile strength-S/N ratio analysis table

Level	T _m , °C	S, Rpm	SiC, Wt. %	TiO ₂ , Wt. %
1	46.1	46.27	48.19	48.43
2	45.03	45.26	46.68	46.55
3	46.2	47.89	45.56	45.64
Delta	0.21	0.48	1.01	0.89
Rank	4	3	1	2

In this study, the Taguchi approach is implemented using MINITAB-21 software, focusing on a "greater is better" S/N ratio for optimal parameter prediction. The response characteristics such as tensile strength and hardness based on the L27 orthogonal array are evaluated. The final hardness and tensile strength values were determined by averaging five

readings from each experiment.

Table 3 presents the response properties and Signal to Noise ratios for four control factors across three levels, following the L27 orthogonal array.

The response table for hardness for the appropriate control parameters is shown in Tables 4 and 5. The impact of input parameters on composite hardness was in the following order: silicon carbide (Wt%), titanium dioxide (Wt%), melt-temperature (°C), and stirring speed (°C/min). Table 5 display the response table for AS21 composite's tensile strength. Silicon carbide (Wt%), titanium dioxide (Wt%), temperature of melt (°C), and speed of stirring (rpm) had greatest effects on tensile strength.

Each control factor levels are assessed using the main effects plot analysis of the Taguchi technique in order to estimate the ideal level of operating parameters for the AS21 hybrid composite's strength and hardness. The primary influence plot of the process parameters for the response characteristics of hardness and tensile strength is shown in Figures 8 and 9 respectively. The S/N ratio analysis revealed that 750°C of melt temperature and 400rpm of stirring speed with 2 Wt% of SiC and 0.5 Wt% of TiO₂ reinforcements were the best process parameters for AS21-SiC-TiO₂ hybrid composite to achieve exceptional mechanical performance.

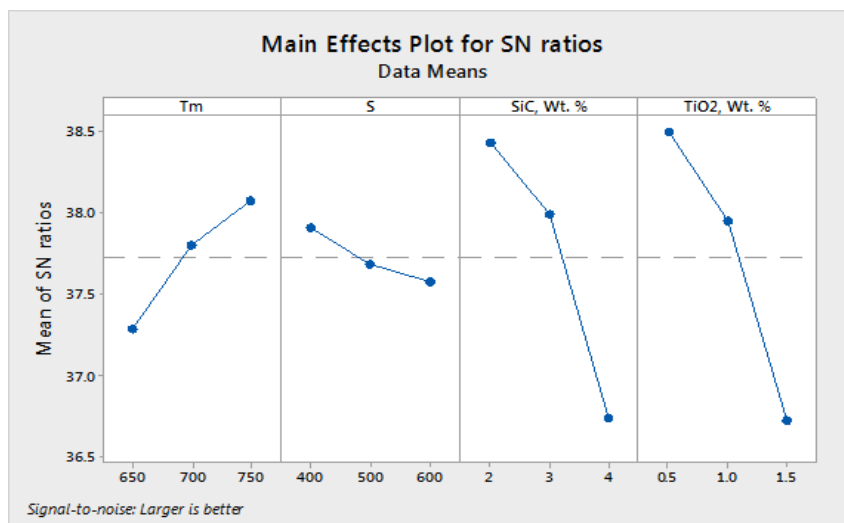


Figure 8. S/N ratio of the control factors taken into consideration and the main effect plot for hardness

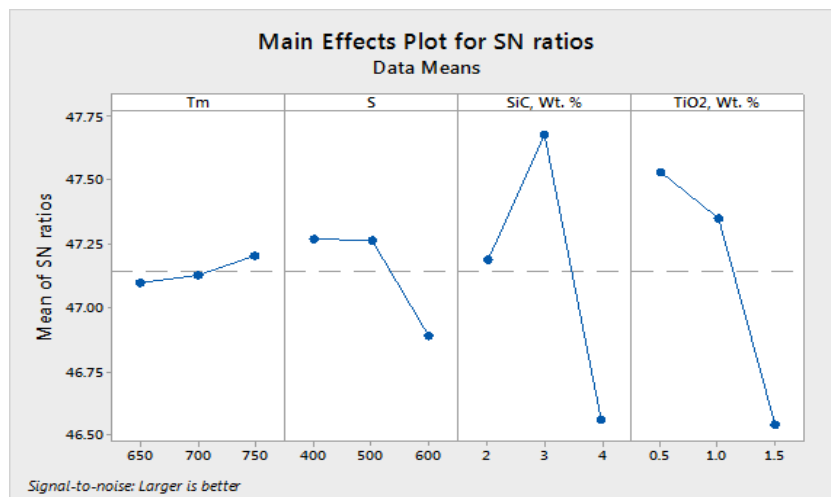


Figure 9. S/N ratio of the control factors taken into consideration and the main effect plot for tensile strength

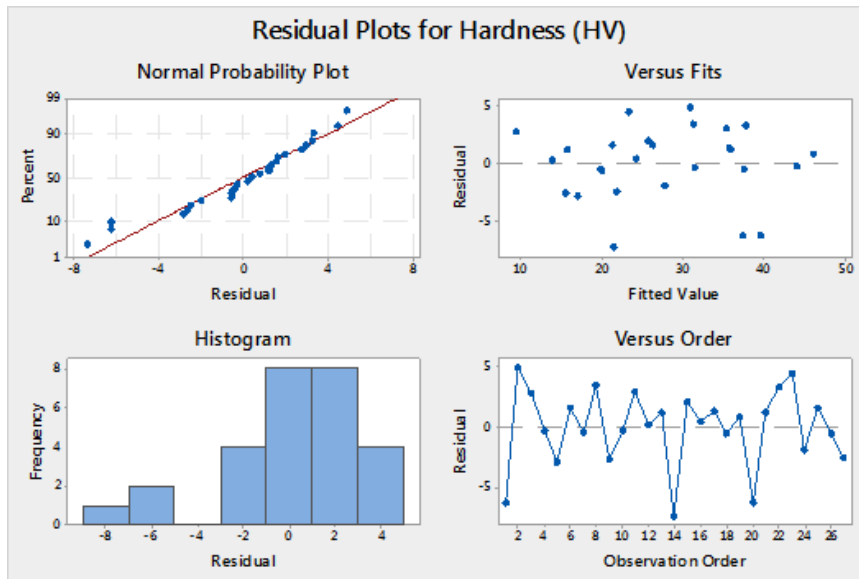


Figure 10. Residual plot for hardness of AS21 hybrid composite

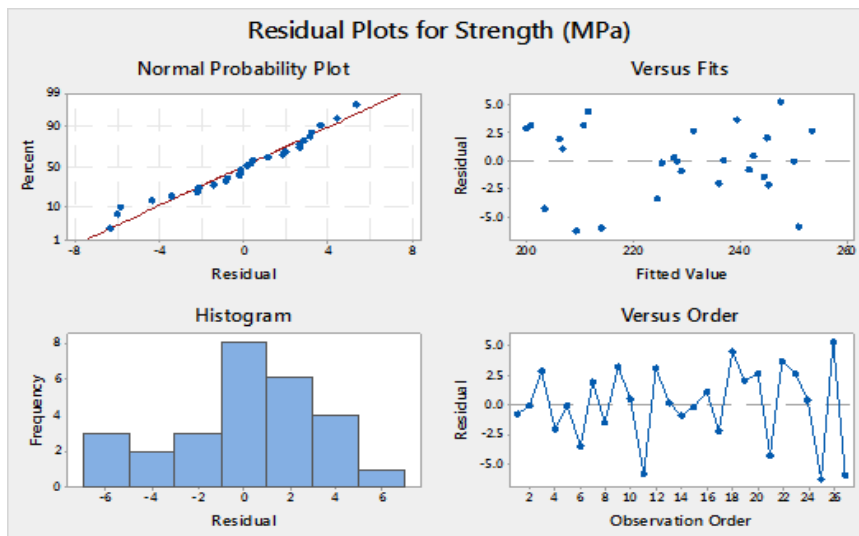


Figure 11. Residual plot for tensile strength of AS21 hybrid composite

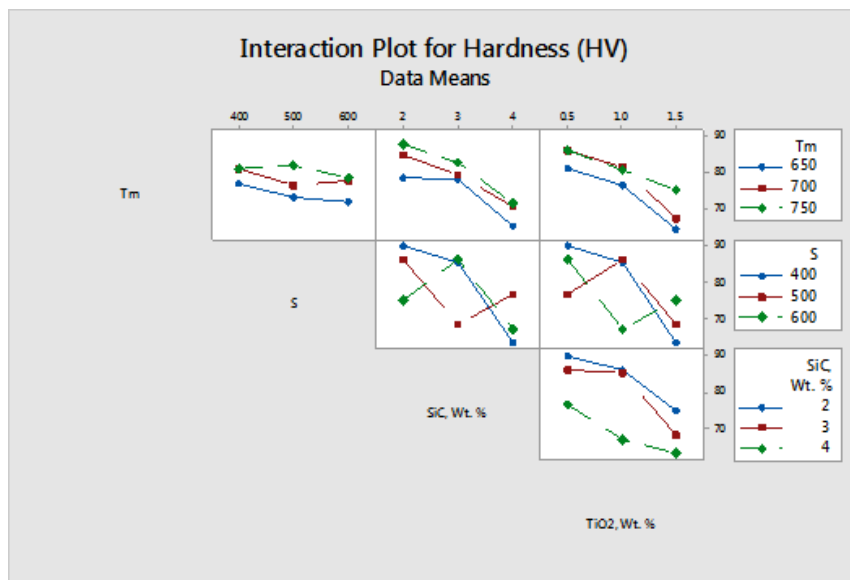


Figure 12. Interaction plot for hardness of AS21 hybrid composite

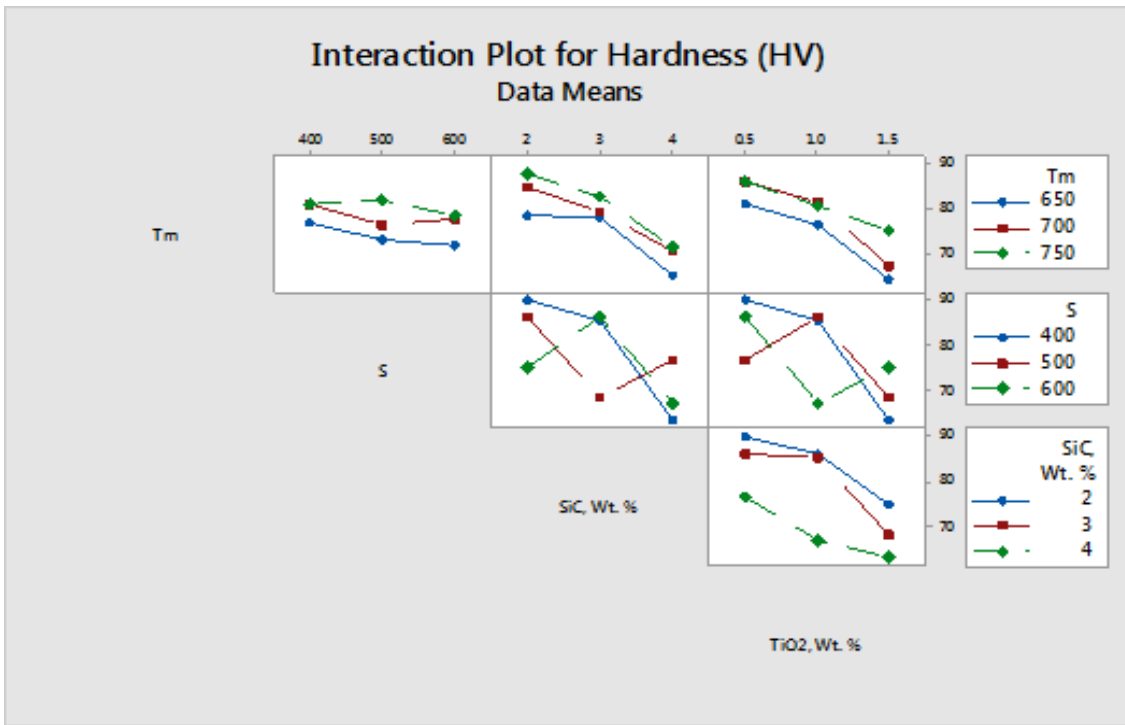


Figure 13. Interaction plot for tensile strength of AS21 hybrid composite

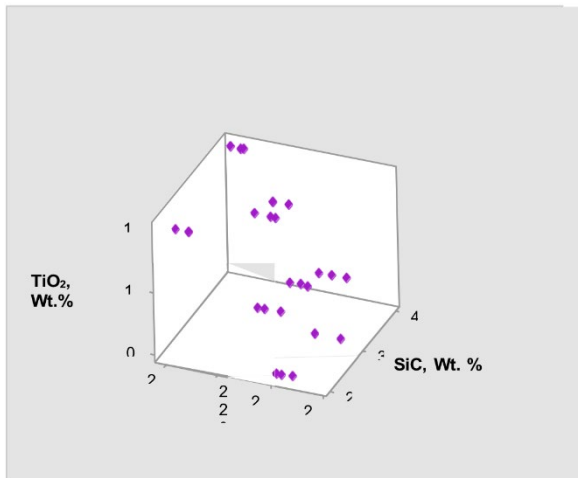


Figure 14. 3D scatter plot of tensile strength Vs SiC and TiO₂

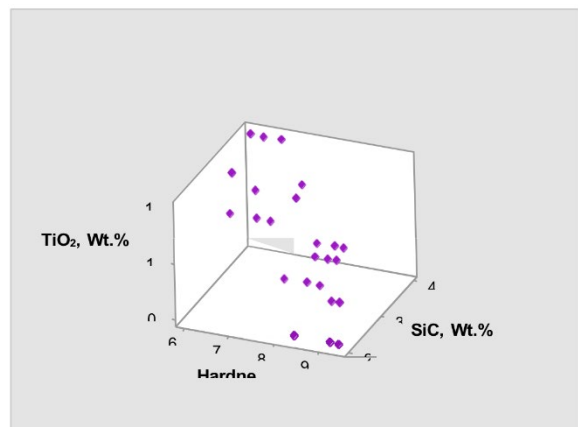


Figure 15. 3D scatter plot of hardness vs SiC and TiO₂

The residual strength and hardness graphs of the AS21 composite are shown in Figures 10 and 11, which further explain the consistency of the experimental data. Since the results are nearer to the center line, the conclusions are trustworthy. The hybrid reinforcements of SiC and TiO₂ are seen to have the greatest influence when compared to other components in the interaction plot of Figures 12 and 13. The 3D scatter plot of mechanical characteristics in relation to hybrid reinforcement in AS21 alloy is shown in Figures 14 and 15. The combination of 0.5% titanium dioxide and 2% silicon carbide was found to produce the maximum hardness. On the other hand, the mixture of 1% titanium dioxide and 3% silicon carbide showed greater tensile strength.

3.6 Anova results

The relevance of each control factor on various quality indicators is predicted using an ANOVA analysis. The importance of input component on the response properties of hardness is displayed in Table 6. SiC reinforcement has got second place with a contribution of 38.43%, making TiO₂ reinforcement the most important factor in the measurement of hardness. On the tensile strength measurement shown Table 7, SiC reinforcement contributes the most (47.71%), followed by TiO₂ reinforcement (41.27%). SiC reinforcement and TiO₂ reinforcement are the main factors that significantly influence the AS21 hybrid composites mechanical characteristics, it should be emphasized. Additionally, the study reveals that the R² value is greater than 90%, showing that the outcomes are only satisfactory. Therefore, hybrid reinforcement has a clear impact on AS21 hybrid composites mechanical characteristics. The interaction and scatter graphs in Figures 12-15 support the same.

Table 6. Hardness analysis-ANOVA

Source	DoF	Seq SS	Contribution	Adj SS	Adj MS	F Value	P Value
T _m , (°C)	2	192.66	6.08%	192.66	95.83	6.82	0.006
S, (rpm)	2	98.7	4.54%	98.7	48.85	3.51	0.052
SiC, Wt.%	2	1074.99	38.43%	1074.99	547.99	38.91	0
TiO ₂ , Wt.%	2	1112.86	41.51%	1111.86	545.43	38.14	0
Error	18	254.42	8.34%	254.42	13.19		
Total	26	2734.62	100%				

S=3.76695; R-sq=90.66%; R-sq, adj=86.51%;

Table 7. Tensile strength-ANOVA

Source	DoF	Seq SS	Contribution	Adj SS	Adj MS	F Value	P Value
T _m , (°C)	2	51.89	0.63%	50.89	25.44	1.71	0.209
S, (rpm)	2	556.22	7.05%	556.22	273.11	19.03	0.000
SiC, Wt. %	2	3730.22	47.71%	3730.22	1915.11	127.73	0.000
TiO ₂ , Wt. %	2	3213.56	41.27%	3213.56	1556.78	112.37	0.000
Error	18	268.78	3.34%	257.78	13.88		
Total	26	8027.67	100%				

S = 3.85701; R-sq = 96.66%; R-sq, adj = 95.18%;

3.7 Regression equations

Multiple linear regression equations are designed to predict the relationship between response characteristics and input factors such as melt temperature (T_m), stirring speed (rpm), SiC reinforcement (Wt.%) and TiO₂ reinforcement (Wt.%) using the MINITAB software. Regression Eqs. (1) and (2) computed for response characteristics are as follows.

$$\begin{aligned}
 \text{Hardness(HV)} &= 77.1 + 0.0667T_m - 0.0172S \\
 &\quad - 7.39\text{Wt. \% of SiC} \\
 &\quad - 15.44\text{Wt. \% of TiO}_2
 \end{aligned}
 \tag{1}$$

$$\begin{aligned}
 \text{TensileStrength(MPa)} \\
 &= 281.0 + 0.0322T_m - 0.0511S \\
 &\quad - 8.11\text{Wt. \% of SiC} \\
 &\quad - 25.44\text{Wt. \% of TiO}_2
 \end{aligned}
 \tag{2}$$

3.8 Confirmation test

After determining the best input process parameters, validations experiments were conducted to determine the accuracy of the best combination as well as other combinations which are shown in Table 8. The mechanical parameters of AS21 composite as expected and as measured are shown in Table 9. The Taguchi optimization yields a very low variation with an error of 1.64%, demonstrating strong concurrence.

Table 8. Confirmation experiments

S. No	T _m (°C)	S (rpm)	SiC (Wt.%)	TiO ₂ (Wt.%)
1	650	400	3	1.0
2	700	400	2	0.5
3	750	400	2	0.5
4	750	600	3	0.5

Table 9. Confirmation experiment results

S. No	Hardness (HV)		Error (±%)	Tensile Strength (MPa)		Error (±%)
	Experimental	Predicted.		Experimental	Predicted.	
1	85.06	85.42	0.42	248.54	246.66	0.75
2	92.54	92.34	0.32	246.36	249.74	1.46
3	94.65	92.11	1.64	246.89	247.52	1.06
4	89.02	88.29	1.43	242.64	258.82	1.41
5	91.06	90.56	1.50	244.24	249.23	1.25
6	87.41	89.23	1.21	251.51	252.05	1.54
7	92.69	92.54	0.54	248.84	258.45	1.08
8	90.44	89.65	1.28	245.25	249.53	1.05
9	89.69	87.56	1.54	244.66	256.77	1.14
10	88.56	89.54	1.31	253.63	259.96	1.25

4. CONCLUSIONS

The following conclusions emerged from the present research:

- Taguchi DOE was successfully implemented to improve the mechanical properties of AS21 Mg alloy reinforced with SiC-TiO₂ hybrid particulates.
- The S/N ratio analysis of hardness data reveals that the maximum hardness of 94 HV was attained with optimized parameters: temperature of melt 750°C, a

stirring speed of 400 rpm, and reinforcements of 2 wt% SiC and 0.5 wt% TiO₂.

- For tensile strength, the optimal parameters resulted in a greater strength of 253MPa, using the same melt temperature and stirring speed, but with 3 wt% SiC and 0.5 wt% TiO₂.
- ANOVA results for hardness revealed that TiO₂ reinforcement has the most significant effect, contributing 40.61% to the hardness of the composite.
- Conversely, ANOVA for tensile strength indicated

that SiC reinforcement is more influential, contributing 47.71% to the tensile strength.

- The variation of control factors in the AS21 Mg alloy hybrid composite was quantitatively modelled using regression equations.
- The hardness of the composites enhanced with the addition of SiC reinforcement and melt temperature. Adding 2-6 wt.% of SiC enhanced the hardness of the AS21 alloy by 10.67% and 28.35%, respectively. The best combination of parameters for achieving the highest hardness in AS21/SiC composites are estimated to be 6 wt.% SiC, a melt temperature of 700°C, and speed of stirring 500rpm.
- A confirmation test showed strong agreement between actual and expected mechanical properties, with a discrepancy of only 1.64%.
- Future research will explore different reinforcement combinations, such as 20% SiC and 80% TiO₂, and 30% SiC and 70% TiO₂, improve the alloy's mechanical properties to a greater extent.

REFERENCES

- [1] Song, J., She, J., Chen, D., Pan, F. (2020). Latest research advances on magnesium and magnesium alloys worldwide. *Journal of Magnesium and Alloys*, 8(1): 1-41. <https://doi.org/10.1016/j.jma.2020.02.003>
- [2] Saberi, A., Bakhsheshi-Rad, H.R., Karamian, E., Kasiri-Asgarani, M., Ghomi, H. (2020). Magnesium-graphene nano-platelet composites: Corrosion behavior, mechanical and biological properties. *Journal of Alloys and Compounds*, 821: 153379. <https://doi.org/10.1016/j.jallcom.2019.153379>
- [3] Deng, K.K., Wang, X.J., Wang, C.J., Shi, J.Y., Hu, X.S., Wu, K. (2012). Effects of bimodal size SiC particles on the microstructure evolution and fracture mechanism of AZ91 matrix at room temperature. *Materials Science and Engineering: A*, 553: 74-79. <https://doi.org/10.1016/j.msea.2012.05.094>
- [4] Rao, D.R., Srinivas, C. (2022). Empirical modelling and multi-objective optimisation of laser micro machining on magnesium alloy AS21-SiC metal matrix composite. *Annales de Chimie - Science des Matériaux*, 46(5): 259-271. <https://doi.org/10.18280/acsm.460505>
- [5] Braszczyńska-Malik, K.N., Zyska, A. (2010). Influence of solidification rate on microstructure of gravity cast-AZ91 magnesium alloy. *Archives of Foundry Engineering*, 10(1): 23-26.
- [6] Poddar, P., Srivastava, V.C., De, P.K., Sahoo, K.L. (2007). Processing and mechanical properties of SiC reinforced cast magnesium matrix composites by stir casting process. *Materials Science and Engineering: A*, 460: 357-364. <https://doi.org/10.1016/j.msea.2007.01.052>
- [7] Ong, T.H.D., Yu, N., Meenashisundaram, G.K., Schaller, B., Gupta, M. (2017). Insight into cytotoxicity of Mg nanocomposites using MTT assay technique. *Materials Science and Engineering: C*, 78: 647-652. <https://doi.org/10.1016/j.msec.2017.04.129>
- [8] Jia, X.Y., Liu, S.Y., Gao, F.P., Zhang, Q.Y., Li, W.Z. (2009). Magnesium matrix nanocomposites fabricated by ultrasonic assisted casting. *International Journal of Cast Metals Research*, 22(1-4): 196-199. <https://doi.org/10.1179/136404609X367704>
- [9] Luo, A.A. (2013). Magnesium casting technology for structural applications. *Journal of Magnesium and Alloys*, 1(1): 2-22. <https://doi.org/10.1016/j.jma.2013.02.002>
- [10] Guo, W., Wang, D., Fu, Y., Zhang, L., Wang, Q. (2016). Dry sliding wear properties of AZ31-Mg 2 Si magnesium matrix composites. *Journal of Materials Engineering and Performance*, 25: 4109-4114. <https://doi.org/10.1007/s11665-016-2263-5>
- [11] Elumalai, P.C., Ganesh, R. (2020). Synthesis and characterisation of magnesium matrix composite reinforced with titanium dioxide nanoparticulates. *Materials Research Express*, 7(1): 015093. <https://doi.org/10.1088/2053-1591/ab6ca3>
- [12] Natarajan, P., Jegan, A., Mohanraj, M. (2020). Wear behavior of Ni-TiO₂ nano-composite coating on AISI 1022 CS by pulse electrodeposition. *Journal of New Materials for Electrochemical Systems*, 23(3): 177-181. <https://doi.org/10.14447/jnmes.v23i3.a04>
- [13] Deng, K.K., Wang, C.J., Nie, K.B., Wang, X.J. (2019). Recent research on the deformation behavior of particle reinforced magnesium matrix composite: A review. *Acta Metallurgica Sinica (English Letters)*, 32: 413-425. <https://doi.org/10.1007/s40195-019-00872-9>
- [14] Aathisugan, I., Rose, A.R., Jebadurai, D.S. (2017). Mechanical and wear behaviour of AZ91D magnesium matrix hybrid composite reinforced with boron carbide and graphite. *Journal of Magnesium and Alloys*, 5(1): 20-25. <http://doi.org/10.1016/j.jma.2016.12.004>
- [15] Narayanasamy, P., Selvakumar, N. (2017). Tensile, compressive and wear behaviour of self-lubricating sintered magnesium based composites. *Transactions of Nonferrous Metals Society of China*, 27(2): 312-323. [https://doi.org/10.1016/S1003-6326\(17\)60036-0](https://doi.org/10.1016/S1003-6326(17)60036-0)
- [16] Karthick, E., Mathai, J., Tony, J.M., Marikkannan, S.K. (2017). Processing, microstructure and mechanical properties of Al₂O₃ and SiC reinforced magnesium metal matrix hybrid composites. *Materials Today: Proceedings*, 4(6): 6750-6756. <https://doi.org/10.1016/j.matpr.2017.06.451>
- [17] Rognatha Rao, D., Srinivas, C. (2023). Influence of Nano-SiC reinforcement during laser cutting of magnesium AS21-Bimodal SiC composites. *Advances in Materials and Processing Technologies*, 1344-1366. <https://doi.org/10.1080/2374068X.2023.2189678>
- [18] Balak, Z., Zakeri, M. (2016). Application of Taguchi L32 orthogonal design to optimize flexural strength of ZrB₂-based composites prepared by spark plasma sintering. *International Journal of Refractory Metals and Hard Materials*, 55: 58-67. <http://doi.org/10.1016/j.ijrmhm.2015.11.009>
- [19] Babu, K.A., Jeyapaul, R. (2022). An investigation into the wear behaviour of a hybrid metal matrix composite under dry sliding conditions using Taguchi and ANOVA methods. *Journal of Bio-and Tribo-Corrosion*, 8(1): 15. <https://doi.org/10.1007/s40735-021-00608-2>
- [20] Elumalai, P.C., Radhakrishnan, G., Emarose, S. (2021). Investigation into physical, microstructural and mechanical behaviour of titanium dioxide nanoparticulate reinforced magnesium composite. *Materials Technology*, 36(10): 575-584. <https://doi.org/10.1080/10667857.2020.1782050>
- [21] Meenashisundaram, G.K., Nai, M.H., Almajid, A., Gupta, M. (2015). Development of high performance Mg-TiO₂

nanocomposites targeting for biomedical/structural applications. *Materials & Design* (1980-2015), 65: 104-114. <https://doi.org/10.1016/j.matdes.2014.08.041>

[22] Meenashisundaram, G.K., Nai, M.H., Gupta, M. (2015). Effects of primary processing techniques and

significance of hall-petch strengthening on the mechanical response of magnesium matrix composites containing TiO₂ nanoparticulates. *Nanomaterials*, 5(3): 1256-1283. <https://doi.org/10.3390/nano5031256>